第 26卷 第 9期 焊 接 学 报 Vol. 26 No. 9
2005年 9月 TRANSACTIONS OF THE CHINA WELDING INSTITUTION September 2005

全焊接阀门的焊接温度场拟合分析

庞方杰[1], 徐济进[1], 陈立功[1], 张 敏[2]
(1. 上海交通大学 材料科学与工程学院, 上海 200030;
2. 上海耐莱斯·詹姆斯伯雷阀门有限公司, 上海 200092)

摘 要: 建立了一种基于试验的非线性曲线拟合的新方法来分析焊接温度场。采用改进的温度场数学解析模型后, 拟合得到与实测结果相当接近的温度 – 时间拟合曲线方程。根据不同条件下的拟合方程, 对其回归系数进行了影响因素的分析。并考虑实际需要, 得到了不同初始温度下全焊接阀体的密封圈安全位置范围, 为阀门焊接工艺的制定提供了重要依据。

关键词: 全焊接阀门; 温度场; 曲线拟合
中图分类号: TG402 文献标识码: A 文章编号: 0253-360X(2005)09-73-04

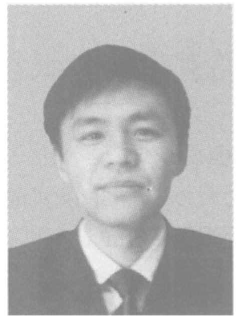

庞方杰

0 序 言

"西气东输"项目需要使用大量大直径球阀, 对于油气介质, 球阀密封性是首先要解决的问题, 由于密封性能差产生的泄漏会导致严重的环境污染和经济损失。而阀门强度的不足则可能造成阀门本体或系统的破坏[1]。采用比螺栓连接阀门具有更多优点的全焊接球阀可有效地解决上述难题。

试验采用国内第一台单电源双丝自动埋弧焊机进行平板试样的焊接。单电源双丝埋弧自动焊是一种高熔敷速率、高焊接速度、低热输入的埋弧焊方法。通过改变焊丝排列方式和丝间距, 其焊缝成形、熔深、熔宽、稀释率可得到更充分的调节。既可用于稀释率要求较低的耐磨或耐腐蚀表面的埋弧堆焊, 亦可适用于各种对接、角接焊缝的单道或多道高速埋弧焊[2]。

全焊接阀门焊接过程中, 阀体需要用橡胶圈进行密封, 这给阀门结构设计和实际焊接带来了一定困难。一方面阀体在焊接时温度较高, 另一方面密封圈耐温较低, 因此必须建立特殊的温度控制工艺。为此首先需要了解模拟阀体的平板试样的焊接温度场影响因素及其随时间的变化曲线, 这里采用拟合法将试验采集到的温度数据进行分析, 得到符合规律的温度 – 时间关系式; 进一步获取不同位置的最高温度及其影响因素, 从而为确定阀门密封圈的位置范围提供依据。实测温度场数据为由热电偶测得的垂直于焊缝中心的焊接试样表面温度值。

收稿日期: 2004-10-18

1 焊接温度场模型的选取

平板对接焊试样如图 1所示, 其在三个方向的长度都不能忽略, 考虑到密封圈位置不在焊缝和热影响区, 这里参考了 Rosenthal解析模型。

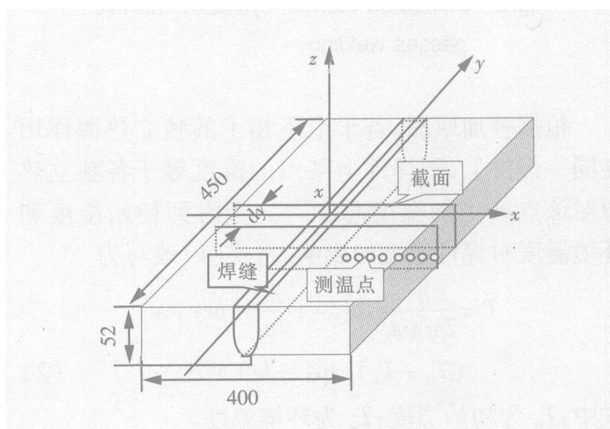

图 1 平板对接焊示意图

Fig. 1 Configuration of flat plate for butt welding

对于厚大焊件连续移动热源的温度场, 可将焊件划分为一个个垂直焊缝的截面, 并假定相邻截面薄片之间不发生热交换, 仅在垂直于焊道方向有热传播, 因此可以这样认为, 只有在热源到达该薄片时才传热。如果薄片的厚度为 dy, 就可以把厚大焊件点状热源的传热过程看作是在厚度为 dy 薄片一边有瞬时线状热源作用的传热过程[3]。考虑表面散

热时,其温度解析式的一个特解为

$$T=\frac{q}{2\pi\lambda vt}\exp[-(\frac{r^2}{4at}+bt)]+T_e \quad (1)$$

试中: a 为被焊材料的导温系数; λ 为导热系数; q 为热源功率; v 为焊接速度; t 为时间; b 为散热系数; r 为距焊缝中心的距离 ($r^2=x^2+z^2$); T_e 为环境温度。

2 实测曲线与拟合分析

2.1 模型改进

用温度场测量仪实时测量了对接焊试样中心截面上距焊缝 30 mm 处的下表面温度。可以看到,随着起焊温度的提高,测点温度也相应提高 (见图 2)。

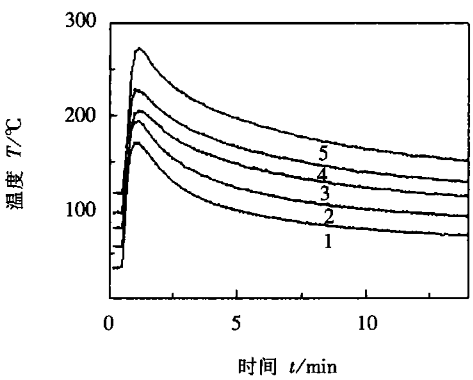

图 2 前 5道焊接的温度 –时间曲线

Fig. 2 Measured thermal cycles in first five passes welding

根据叠加原理,若干个不相干的独立热源作用在同一焊件上,则焊件上某点的温度等于各独立热源对该点产生的温度总和[3]。考虑到初始温度和环境温度对焊件温度的影响,将式(1)改写为

$$T=\frac{q}{2\pi\lambda vt}\exp[-(\frac{r^2}{4at}+bt)]+(T_0-T_e)\exp(-bt)+T_e \quad (2)$$

式中: T_0 为初始温度; T_e 为环境温度。

2.2 拟合方程

由于式(2)中的一些热学参数受温度等因素影响变化较大,并非为确定常数,再加上模型本身假定条件的限制,不可能直接使用式(2)来计算焊接试样的温度场。

这里使用曲线拟合的方法来获得与实际试样温度曲线相符合的温度表达式。将式(3)通过数学工具软件来进行拟合,其中 P_1、P_2、P_3 为回归系数。

$$T(t)=\frac{P_1}{t}\exp[-(\frac{P_2}{t}+P_3t)]+(T_0-T_e)\exp(-P_3t)+T_e \quad (3)$$

图 3为双丝多道埋弧焊焊接过程中某一道焊接时的温度 –时间曲线图,图中从上往下依次为距焊缝中心 0 mm、45 mm、65 mm、85 mm、105 mm、125 mm、145 mm、165 mm 处的温度 –时间曲线。图 4为相应拟合曲线。由于该温度场模型在焊缝中心处偏差较大,故图 4中 0 mm 的起始段温度偏高。从图 3、4可看到拟合的曲线与实测曲线相当符合。

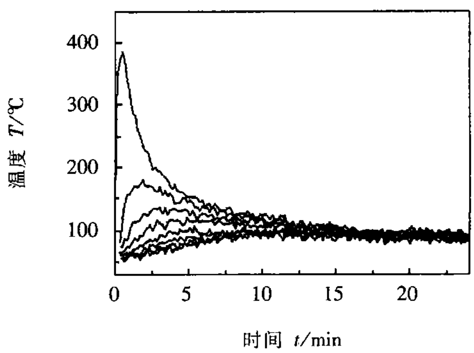

图 3 实测的温度 –时间曲线

Fig. 3 Measured thermal cycles of eight locations

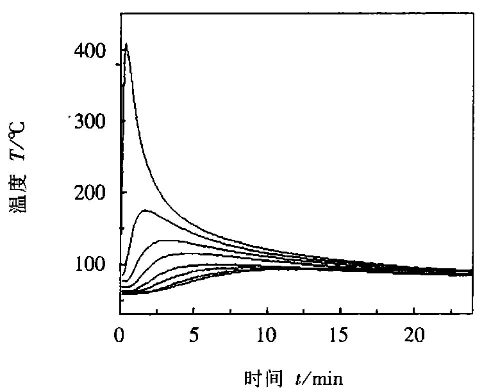

图 4 拟合后的温度 –时间曲线

Fig. 4 Fitted thermal cycles of eight locations

2.3 回归系数的影响因素分析

将每次得到的温度 –时间曲线进行拟合,可以发现回归系数 P_1、P_2、P_3 受焊接条件的影响呈规律性变化。

尽管实际焊接时输入的热源功率变化不大,然而拟合结果发现参数 P_1 却明显随测点距焊缝距离的增加而增大(见表 1)。

参数 P_2 随测点距热源距离的增加而提高;图 5为热源与测点在 z 方向距离为 26 mm(第 7道焊接)时各测点的 P_2 值与 x^2+z^2 的关系图。从图中可以看出其线性性较好,这与解析式(2)中的 $-r^2/4at$ 项相吻合。由此可进一步求出此时的导温系数 a。

表 1　测点位置与参数 P_1 的对应表

Table 1　Locations of measuring points and regression coefficient P_1

测点位置 x /mm	0	45	65	85	105	125	145	165
参数 P_1	705	828	911	958	1 188	1 245	1 264	1 620

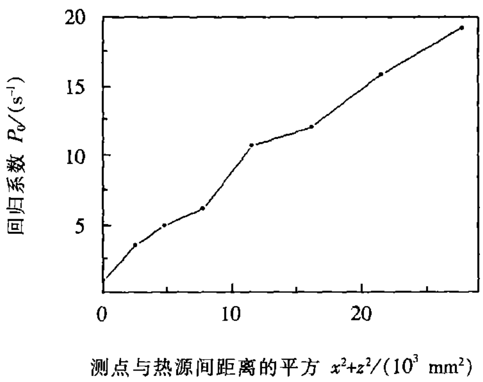

图 5　回归系数 P_2 与测点热源间距离的关系

Fig. 5　Effect of distance between heat source and measuring points on regression coefficient P_2

试验发现，参数 P_3 与初始温度和冷却条件有关。它随 T_0 的增加而增加（见表 2）；同时，若用风冷来加快试样表面的对流时，P_3 的值也会有进一步的增加。可以认为这是一个与散热能力相关的参数。

表 2　初始温度 T_0 与参数 P_3 的影响表

Table 2　Initial temperatures and regression coefficient P_3

初始温度 T_0 /℃	34	57	75	90	109
参数 P_3	−0. 01	−0. 007	−0. 001	0. 000 1	0. 004

3　结果分析

当试样初始温度为 70 ℃时，由拟合曲线方程计算到的极点，计算出不同位置的最高温度（极点处温度）同其所在位置的 $T_{max}-x$ 关系曲线（见图 6实线部分），可发现这与根据实测结果得到的 $T_{max}-x$ 曲线非常接近（见图 6虚线部分）。随 x 的增加，T_{max} 呈递减趋势。考虑到密封圈耐热极限温度为 120 ℃；在初始焊接温度为 70 ℃时，由计算曲线得到满足 $T_{max}<120$ ℃的 x 最小值为 76 mm。

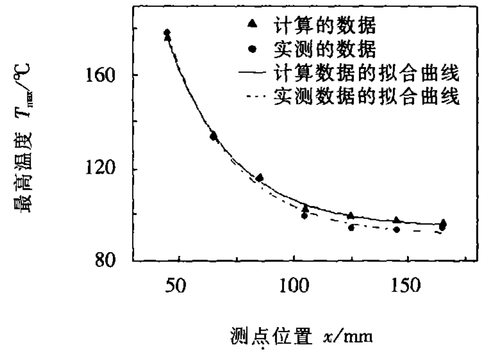

图 6　$T_0=70$ ℃，实测与计算的 $T_{max}-x$ 的曲线

Fig. 6　Measured and calculated $T_{max}-x$ curve ($T_0=70$ ℃)

同样，当试样初始焊接温度为 80 ℃时，相应的 $T_{max}-x$ 关系曲线见图 7，也可由计算曲线得到满足 $T_{max}<120$ ℃的 x 最小值为 80mm。

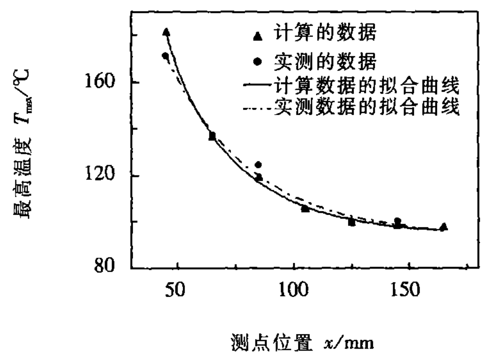

图 7　$T_0=80$ ℃，实测与计算的 $T_{max}-x$ 曲线

Fig. 7　Measured and calculated $T_{max}-x$ curve ($T_0=80$ ℃)

由此进一步得出，在相同焊接条件及冷却环境下，符合 $T_{max}<120$ ℃的 x 最小值 x_{min} 与焊接试样初始温度 T_0 的关系曲线（见图 8）。

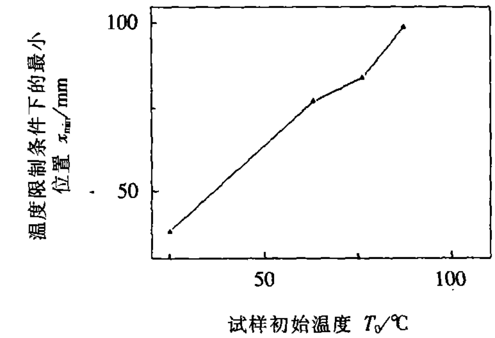

图 8　T_0-x_{min} 的关系曲线

Fig. 8　Curve of T_0-x_{min}

焊接工艺确定了试样的初始温度 T_0 后,可再次利用得到的温度 – 时间拟合方程计算出每一道焊接后所需的冷却时间;从而为制定完整的温度控制工艺提供依据。

4 结 论

根据试验的要求,建立了符合温度实测结果的数学模型,并通过曲线拟合来获取拟合方程的各个参数,进而分析得到试样焊接参数对回归系数的影响。可以从结果发现,在试样初始温度为 80 ℃时,密封圈的位置区间仍然较大(x> 80 mm),能够满足阀体密封圈的安放要求。

参考文献:

[1] 米力田. 油气专用阀门的现状及发展方向[J]. 天然气与石油, 1995, 13(1): 20–24

[2] 何德孚, 华大龙, 陈立功, 等. 单电源双丝埋弧自动焊研究[J]. 电焊机, 2004, 34(增刊): 156–160

[3] 吴德海, 任家烈, 陈森灿. 近代材料加工原理[M]. 北京: 清华大学出版社, 1997.

[4] Ramirez A J, Brandi S D. Application of discrete distribution point heat source model to simulate multipass weld thermal cycles in medium thick plates[J]. Science and Technology of Welding and Joining, 2004, 9(1): 72–82

作者简介:庞方杰,男,1981年出生,硕士研究生。主要从事焊接测量系统的研究,发表论文 2篇。

Email: pangfj@sjtu.edu.cn

[上接第 72页]

固相都视为液相的办法,解决了熔池在形成过程中的熔化区和非熔化区的移动边界问题。

(4) 基于电弧 – 熔池统一数学模型,电弧与熔池不断交互耦合计算得出的熔池形状与试验所得的熔池形状比较吻合。

参考文献:

[1] Choo R T C, Szekely J, Westhoff R C. On the calculation of the free surface temperature of gas tungsten-arc weld pools from first principles, Part I modeling the welding arc[J]. Metallurgical and Materials Transaction B, 1992, 23B(3): 357–369.

[2] Choo R T C, Szekely J, Westhoff R C. On the calculation of the free surface temperature of gas tungsten-arc weld pools from first principles, Part II modeling the weld pool and comparision with experiments[J]. Metallurgical and Materials Transaction B, 1992, 23B(3): 371–384.

[3] Kim W H, Fan H G, Na S J. A mathematical model of gas tungsten arc welding considering the cathode and the free surface of the weld pool[J]. Metallurgical and Materials Transactions B, 1997, 28B(8): 679–686.

[4] Lin M L, Eagar T W. Influence of surface depression and convection on arc weld pool geometry[J]. Transport Phenomena in Materials Processing, ASME PED, 1983, 10(1): 63–69.

[5] Cao Zhengning, Wu Chuansong, Wu Lin. Mathematical moding of TIG molten pool with full penetration[J]. Transactions of the China Welding Institution, 1996, 17(1): 62–69.
曹振宁, 武传松, 吴 林, 等. TIG焊接熔透熔池的数学模型[J]. 焊接学报, 1996, 17(1): 62–69.

[6] Zhang Y M, Cao Z N. Numerical analysis of fully penetrated weld pools in gas tungsten arc welding[J]. Proc Instn. Mech Engrs: Part C: Journal of Mechanical Engineering Science, 1996, 210(2): 187–195.

[7] Fan H G, Tsai H L, Na S J. Heat transfer and fluid flow in a partially or fully penetrated weld pool in gas tungsten arc welding[J]. International Journal of Heat and Mass Transfer, 2001, 44(2): 417–428.

[8] Li Z Y, Wu C S. Analysis of the transport phenomena in the interfacial region between TIG arcs and weld pools[J]. Computational Materials Science, 1997, 8(3): 243–250.

[9] 孙俊生, 武传松. 熔池表面形状对电弧电流密度分布的影响[J]. 物理学报, 2000, 49(12): 2427–2432.

[10] Lu Fenggui, Yao Shun, Lou Songnian, et al. Effects of weld pool surface deformation on behavior characters of welding arc[J]. Transations of the China Welding Institution, 2004, 25(2): 57–60.
芦凤桂, 姚 舜, 楼松年, 等. 熔池表面变形对电弧行为特征的影响[J]. 焊接学报, 2004, 25(2): 57–60.

[11] Wu Chuansong. Computer simulation of three-dimensional convection in traveling MIG weld pool[J]. Engineering Computations, 1992, 9(5): 529–537.

作者简介:芦凤桂,女,1975年出生,工学博士,讲师。主要研究方向为焊接过程模拟及高能束加工及控制,发表论文 12篇。

Email: lfg119@sjtu.edu.cn

the vibratory stress relief (VSR) processing, the tensile-compress cyclic loading was applied. The experimental results showed that the dynamic strain has feature of cyclic creep. Cyclic loading affected the creep and creep speed. The bigger the loading, the bigger the creep and the creep speed, and the longer time that the strain became stable. The residual stresses at weld toe were measured using X-ray diffraction method after different cyclic stress amplitude. According to the experimental results, the cyclic creep mechanism during VSR processing was presented.

Key words: vibratory stress relief; welding; stainless steel; creep; cyclic loading

Effect of pulsed parameters on dynamic simulating waveform of pulsed submerged-arc welding process

GUO Hai-yun[1], LI Huan[2], LIU Qiong[2], WANG Jiong-xiang[3], LIU Xin-quan[3], ZHAO Wei-zhen[3], FU Yu-wen[3] (1. Department of Mechanical Engineering, Tianjin Chinese-German Professional Technology Institute, Tianjin 300191, China; 2. School of Materials Science and Engineering, Tianjin University, Tianjin 300072, China; 3. Department of Manufacturing Technology, Shanghai Boiler Works Company Ltd., Shanghai 200245, China). p61-64

Abstract: Since there are many adjustable parameters in alternative speed wire-feeding pulsed submerged-arc welding process, selection of pulsed parameters on the basis of the simulating model was investigated in this paper. The impact of pulsed frequency, duty factor, peak current and base current were discussed, providing a convenient and intuitionistic means for the selection of optimum parameters in practical experiments and foundation for the application of the pulsed submerged-arc welding method.

Key words: pulsed parameters; alternate wire feed system; pulsed submerged-arc welding; simulating waveform

Research on coated solid-wire for metal argon gas welding

ZHANG Jing-hai, ZHAO Fu-chen, DING Yong-zhong (Luoyang Ship Materials Institute, Henan Luoyang 471039, China). p65-68

Abstract: The characteristics and feasibility of metal argon gas welding with coated solid-wire were researched. A nanometer composite coating was developed, which gave the wire a sound weldability during metal argon gas welding. The welding tests showed that the deposited metal with the coated solid-wire had higher mechanical poperties and cold cracking resistance because of its lower oxygen and diffusible hydrogen content compared to that of TIG welded. It could be concluded that metal argon gas welding with coated solid-wire could be a potential method to weld high strength steels with high efficiency and quality.

Key words: coated solid-wire; metal argon gas welding; welding arc; drop transfer

Stationary numerical simulation on coupling interaction between TIG welding arc and pool

LU Feng-gui, TANG Xin-hua, LI Shao-qing, YAO Shun, LOU Song-nian (School of Materials Science and Engineering, Shanghai Jiaotong University, Shanghai 200030, China). p69-72, 76

Abstract: A moving free interface is formed by interaction between welding arc and weld pool. How to deal with the interface is the key to realize coupling interaction between welding arc and pool. Basing on 3D united mathematical model, interaction between TIG welding arc and pool was numerically simulated in this paper. And the theory of interaction between arc and pool was revealled. The result showed that shape of the calculated weld pool was in agree with that of the experiment.

Key words: free interface; coupling interaction; welding arc and pool; numerical simulation

Fitting analysis on welding temperature field of fully welded valve

PANG Fang-jie[1], XU Ji-jin[1], CHEN Li-gong[1], ZHANG Min[2] (1. School of Materials Science and Engineering, Shanghai Jiaotong University, Shanghai 200030, China; 2. Shanghai Neles-Jamesbury Ltd., Shanghai 200092, China). p73-76

Abstract: Welding temperature field was analyzed by using non-linear curve fit method based on experiments. The fitting temperature-time equation was obtained from actual data with an improved mathematic model. From different fitting equations under different conditions, regression coefficients were also analyzed. Considering the actual need, the location range of the sealing loop was acquired.

Key words: fully welded valve; welding temperature field; non-linear curve fit

Numerical simulation of fluid field and temperature field in plasma torch

ZHANG Yi-shun, DONG Xiao-qiang, LI De-yuan (School of Materials Science and Technology, Shenyang University of Technology, Shenyang 110023, China). p77-80

Abstract: The fluid field and temperature field in plasma torch were simulated by using the finite element analysis. The influence of the torch structure on the velocity of water flow and the turbulence formation was analyzed. On the basis of the analyzed results, the temperature field under different fluid field conditions were calculated. By checking computations of the temperature rise at some key location in the torch, it has been found that the cooling effect of the plasma torch can be obviously improved by changing the water flowing route and water entering direction, and which need not increase the flow volume of the cooling water. The calculated data provided a foundation for the torch design and improvement.

Key words: plasma torch; fluid field; temperature field; simulation